Netherlands Journal of Geosciences / Geologie en Mijnbouw 80 (3-4): 229-241 (2001)

Seismogenic faulting in an area of low seismic activity: Paleoseismicity of the El Camp fault (Northeast Spain)

E. Masana[1], J.A. Villamarín[1], J. Sánchez Cabañero[2], J. Plaza[3] and P. Santanach[1]

[1] Universitat de Barcelona, Dept. Geodinàmica i Geofísica, Zona Universitària de Pedralbes, Barcelona 08028, Spain. E-mail: eula@natura.geo.ub.es, javill@geo.ub.es, santanac@natura.geo.ub.es
[2] Consejo de Seguridad Nuclear, Justo Dorado, 11, Madrid 28040, Spain. E-mail: jsc@csn.es
[3] ENRESA, Emilio Vargas, 7, Madrid 28043, Spain. E-mail: JPLH@enresa.es

Manuscript received: July 2000; accepted: October 2001

Abstract

Given that earthquakes do not occur only along high slip-rate faults, slow moving seismogenic faults should be characterized in order to minimize seismic hazard uncertainties. Although no historical earthquakes related to the El Camp fault have been documented, earlier regional geological analysis and the presence of a fault scarp provide evidence of its activity. A paleoseismological study on the southern part of the fault was performed in accordance with the following steps: 1) geological and geomorphologic analysis focussing on the detection of evidence for the seismogenic behavior of the fault, 2) near fault analysis to select the best trenching sites, and 3) trenching to establish and characterize the paleoseismic events. Different dating procedures were used in regional and trenching analyses (Thermoluminiscence, U/Th, Radiocarbon, Pollen analysis). The seismogenic nature of the fault was established by the presence of liquefaction features related to the fault, and by the presence of colluvial wedges composed of large angular blocks. We identified a segment boundary to the north of the Porquerola creek and we focussed our attention on the southern segment, which was active after 125000 yr. The slip rate in this southern segment is 0.02 mm/yr. A minimum of three seismic events were detected, from young to old: the last event Z took place some time prior to 1195 yr AD, the penultimate event Y between event X and the Holocene, and, finally, event X occurred after 125000 yr and prior to 60000 yr. The recurrence period is between 25000 and 35000 yr, the elapsed time is estimated to be no longer than 3000 yr; and the maximum estimated earthquake considering both the onshore and the offshore part of the fault is Mw 6.7 +/-0,5.

Keywords: Seismogenic fault, Paleoseismicity, Trenching, Liquefaction, Spain.

Introduction

Historical seismicity in Europe is concentrated mainly along the active plate boundaries of the Mediterranean region where high differential plate motion is accommodated by fast slipping faults such as the north Anatolian fault or the normal faults along the Gulf of Corinth. In these areas the historical catalogs cover a long period and can provide information on the entire seismic cycle of the seismogenic faults given their high slip rate. Even in these high slip rate faults, in many cases, the historical catalog is insufficient with the result that the seismic cycle cannot be fully described. Lack of information is an even more important limitation when seismicity must be characterized in areas of low slip rates. This is the case in most parts of Europe where, although the historical catalog is long (in Spain it begins, in some areas, in the XIIth century and is fairly complete from the XVIth century), it does not describe adequately the seismic behavior of slow-moving faults with longer seismic cycles (10^3 to 10^5 yr) than the catalog time-period. There are many examples of large earthquakes occurring along slow moving faults. Examples in Spain are the 1427 earthquakes related to the Amer fault in Catalonia and the 1884 Arenas del Rey earth-

quake, the last destructive earthquake in Spain. Hence, large earthquakes can be triggered by slow slip-rate faults with the result that these faults must be characterized. Until recently the seismic potential of a source was estimated using historical catalogs. This may be adequate only where the catalog is complete and long enough to show at least one entire seismic cycle of the target seismic source. By contrast, if only the historical catalog were considered, some slow moving faults would erroneously be regarded as non seismogenic structures. Paleoseismology yields data that contributes to the seismic characterization of such faults.

Three aspects should be considered when analyzing the seismic hazard of areas with low historical seismicity: 1) the location of active faults, 2) the seismogenic behavior of these faults, and 3) the characterization of their seismic parameters. The detection and location of these faults in large areas is a difficult task when based only on the seismicity of the area given that these faults can be silent during inter-seismic periods. However, the geological approach has proved to be very useful. Geomorphologic analysis is particularly helpful when combined with structural analysis in Quaternary sediments and with the results from different absolute and relative dating methods. These studies also shed light on whether or not faults are able to generate shaking given that they allow us to locate outcrops with liquefaction structures. Geological analysis is especially useful in locating the best suitable areas for paleoseismological analysis and in characterizing the seismic behavior of the fault.

In this paper, we present the paleoseismological results obtained along a historically silent fault: the El Camp fault (Fig. 1). The procedures followed in locating the active faults, determining the seismogenic character of the El Camp fault and in establishing its paleoseismological behavior are reported. Special emphasis is placed on the seismic behavior of the fault since this is a matter of debate in other slow active faults in Europe (Camelbeeck and Meghraoui, 1996, Ahorner, 1996, Camelbeeck et al., 2001).

Geological setting

The El Camp fault

The El Camp fault is part of a NE-SW trending system of en echelon normal faults and half-graben basins arranged sub-parallel to the Catalan coast at the northeastern edge of the Iberian Peninsula: the Catalan coastal ranges. These faults form part of a rift system which began its activity, in the early Eocene, north of the Rhine graben. This system extended southwards through the Rhine and Rhone valleys down to the Iberian Peninsula, where it has been active since the early Miocene before, finally, reaching the African plate (Julivert et al., 1972). The faults along the Catalan coastal ranges behaved as strike-slip and reverse faults during Paleogene compression, and have slipped since the early Miocene as normal faults (Fontboté, 1954, Anadón et al., 1979, Guimerà, 1984, Bartrina et al., 1992, Sàbat et al., 1997). The highest peaks along the ranges reach 1700 m in the Montseny, 1100 m in the El Camp and 1400 m in the Baix Ebre areas (Fig. 2) whereas the top of the basin infilling is at an altitude of 200 to 500 m.

The Catalan coastal ranges constitute the northwestern edge of the Valencia trough extensive system, which extends towards the Balearic islands and which has been active since the early Miocene (Fontboté, 1954, Bartrina et al., 1992).

The El Camp fault dips to the WNW and is formed by two en echelon faults separated by a small right

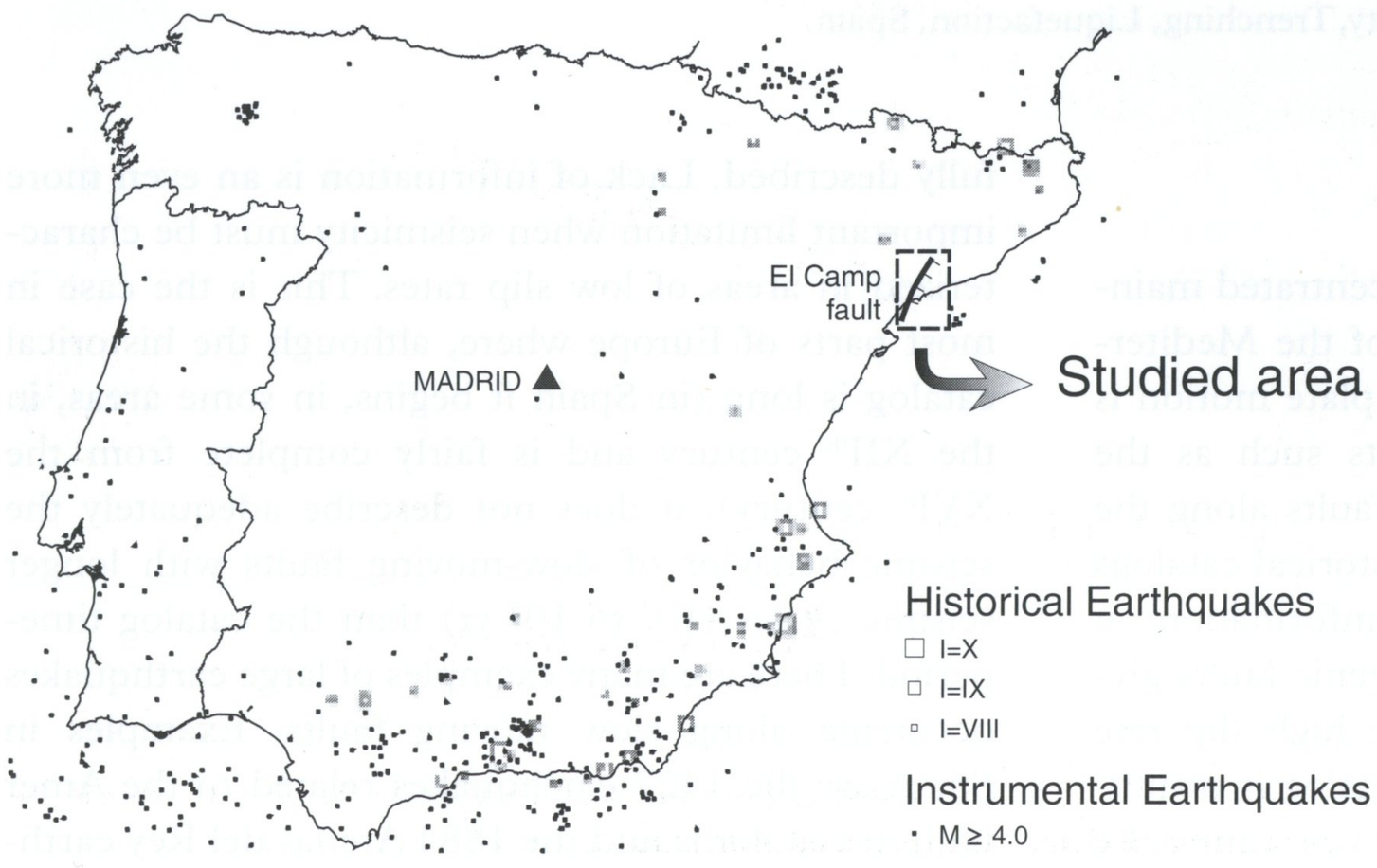

Fig. 1. Seismicity map of the Iberian Peninsula with instrumental earthquakes of magnitudes larger than 4.0 and historical earthquakes with intensities greater than VII (data from Instituto Geográfico Nacional). Seismicity is mainly concentrated in the Betics to the south and in the Pyrenees to the north. The area studied shows no seismicity.

lateral step located near Reus. These faults are referred to as the southern and the northern El Camp faults (Fig. 1and 2). This study focusses on the southern El Camp fault. The half-graben basin which developed next to the fault was filled up in the proximity of the mountain front with terrigenous Miocene deposits which, in the vicinity of Reus (Fig. 2), reach a thickness of 2000 m (Nuñez et al., 1980, Maldonado et al., 1986). Given that the oldest known sediments in the El Camp basin are Burdigalian in age (Anadón et al., 1983) and that the vertical displacement along the fault reaches 3000 m, the vertical slip-rate of the fault approximates 0.16 mm/yr (Masana, 1995).

Seismicity

The seismicity of the Iberian Peninsula (Fig. 1) is considered to be moderate. It is concentrated mainly along the Betics, to the south, with two I=X historical earthquakes (Torrevieja 1829, and Arenas del Rey 1884, data from I.G.N.), and to a smaller extent in the Pyrenees, to the north, with one I=IX-X historical earthquake – Queralbs, 1428 (Banda and Correig, 1984). Apart from these areas, the seismicity in Spain is low. In the Catalan coastal ranges there is infrequent and low-intensity seismicity. Near the El Camp fault the historical catalog begins in the XIIth century, and only one historical earthquake of I>VII is recorded: the Tivissa earthquake (1845). However, it is highly unlikely that this earthquake was triggered by the fault since its epicentral area was located several tens of km to the west of the fault.

Active faults along the Catalan coastal ranges

One of the major problems of using paleoseismological analyses in areas where the catalog does not show large earthquakes is to identify the real sources: it is not possible to perform a complete trenching analysis of all the faults in an area such as the Catalan coastal ranges without a selection of the active faults. A regional geomorphologic analysis is useful in detecting the active faults of an area in a short time. This is done by remote sensing including satellite and aerial photograph analyses, at different scales, together with field work in selected areas. In this study, aerial photographs (1:18000, 1:33000 and 1:70000) as well as topographic maps (1:5000, 1:25000, 1:50000 and 1:250000) of the Catalan coastal ranges were used to perform a geomorphologic analysis of the mountain

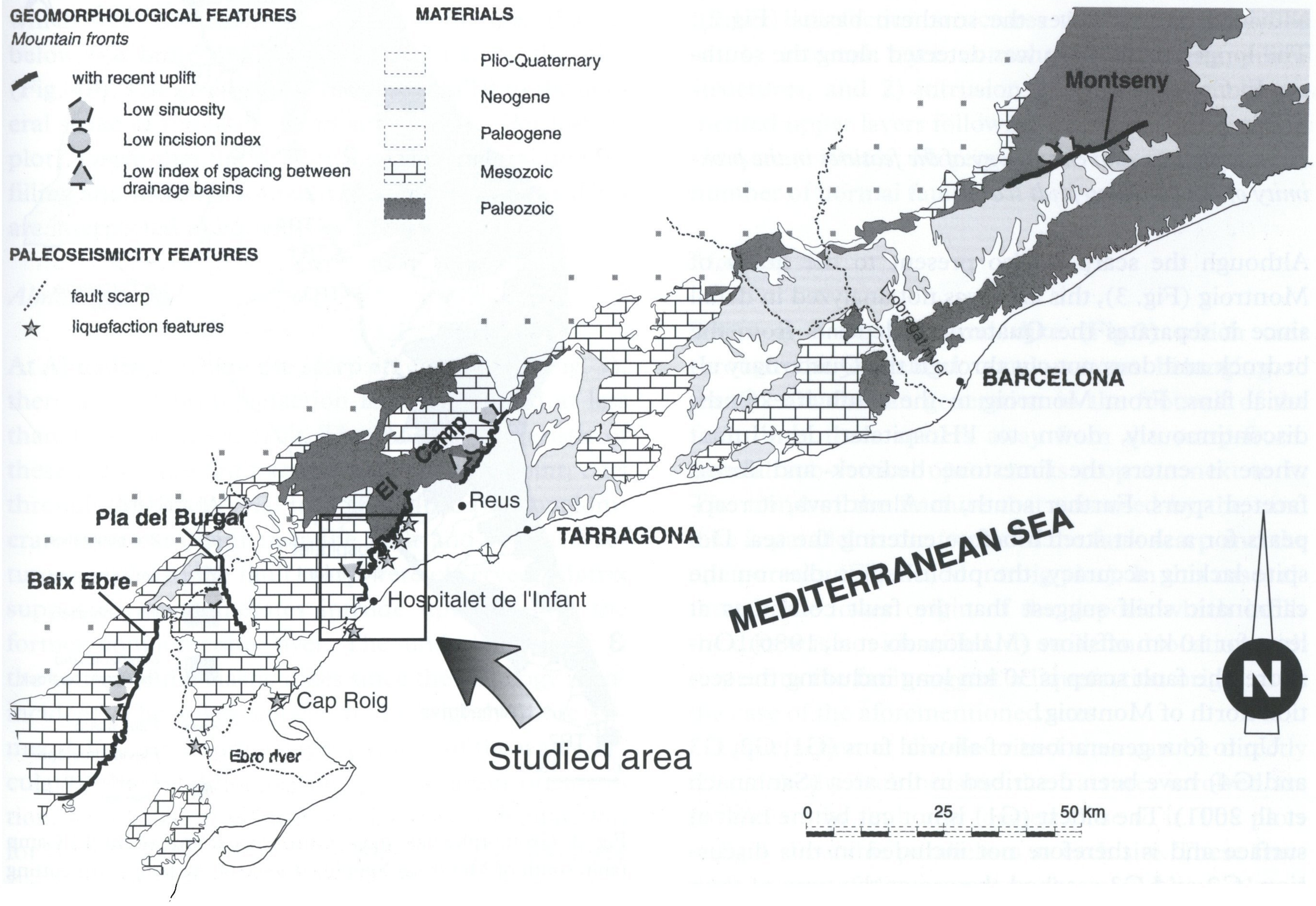

Fig. 2. Geologic map of the Catalan coastal ranges where the El Camp fault is located. Active mountain fronts and fault scarps detected in the zone are indicated. The area studied is centered in the southern El Camp fault (modified from Masana, 1995).

fronts, the fluvial network and the main geomorphologic units of the Quaternary sediments infilling the basins. After selecting some specific areas affected by seismogenic faulting, field work including structural investigations along deformed Quaternary sediments and studies of liquefaction features was carried out.

This study shows that four mountain fronts (Montseny, El Camp, Plà del Burgar and Baix Ebre) are more active than the rest (Fig. 2) given their low sinuosity, low incision index, low index of spacing between drainage basins, convexity along topographic profiles across the front, and well preserved faceted spurs showing different generations, etc (Masana, 1995, 1996). The amount of Quaternary sediments covering the basins is higher in the southern part of the ranges than in the vicinity of the Montseny to the north. Furthermore, in the southern area, deformation of Quaternary sediments is particularly evident: minor faults, tilting of the basin surface towards the mountain front, striated pebbles, liquefaction features, alignments of gradient index anomalies along river profiles, anomalies in the shape of the fluvial network, etc... (Masana, 1994, 1995, 1996). Finally, the main reason for carrying out the paleoseismological study along the El Camp fault was the presence of several fault scarps cutting through the Quaternary alluvial fans that cover the southern basins (Fig.2). The longest fault scarp was detected along the southern El Camp fault.

Geomorphology and chronology of the features in the proximity of the El Camp fault scarp

Although the scarp is also present to the north of Montroig (Fig. 3), this area was not analyzed in detail since it separates the Quaternary deposits from the bedrock and does not cut through the Quaternary alluvial fans. From Montroig to the south it extends, discontinuously, down to l'Hospitalet de l'Infant where it enters the limestone bedrock and forms faceted spurs. Further south, in Almadrava, it reappears for a short stretch before entering the sea. Despite lacking accuracy, the published studies on the carbonatic shelf suggest that the fault continues at least for 10 km offshore (Maldonado et al, 1986). Onshore, the fault scarp is 30 km long including the section north of Montroig.

Up to four generations of alluvial fans (G1, G2, G3 and G4) have been described in the area (Santanach et al. 2001). The oldest (G1) is not cut by the fault at surface and is therefore not included in this discussion. G2 and G3 reached the sea at the time of their deposition and can be correlated with the sea level high-stands, which were their base levels (Fig. 3). No additional units were observed between G2 and G3, and they were correlated with isotopic O stages 9 and 5, respectively. This leads to a deposition age of their top sediments of 300000 and 125000 yr, respectively. As G4 alluvial fans do not reach the sea they cannot be correlated with sea-level high stands. The tops of G2 and G3 fans show well developed calcrete soils that were sampled and dated using the U/Th and Thermoluminiscence methods. Details concerning sampling criteria and the datings are discussed in Villamarín et al. (1999). The results agree with the ages deduced from the correlation of the G2 and G3 top surfaces with the sea-level high stands.

The fault scarp shows a different fault behavior to the north and south of Porquerola creek (Fig.3). To the north, the fault is sealed by the G3 alluvial fans whereas, to the south, it cuts through the G4 alluvial fans. This suggests a segmentation of the El Camp fault. To the north of this creek, the fault did not rupture at surface after 300000 yr and before 125000 yr whereas, to the south, it affected the surface after 125000 yr.

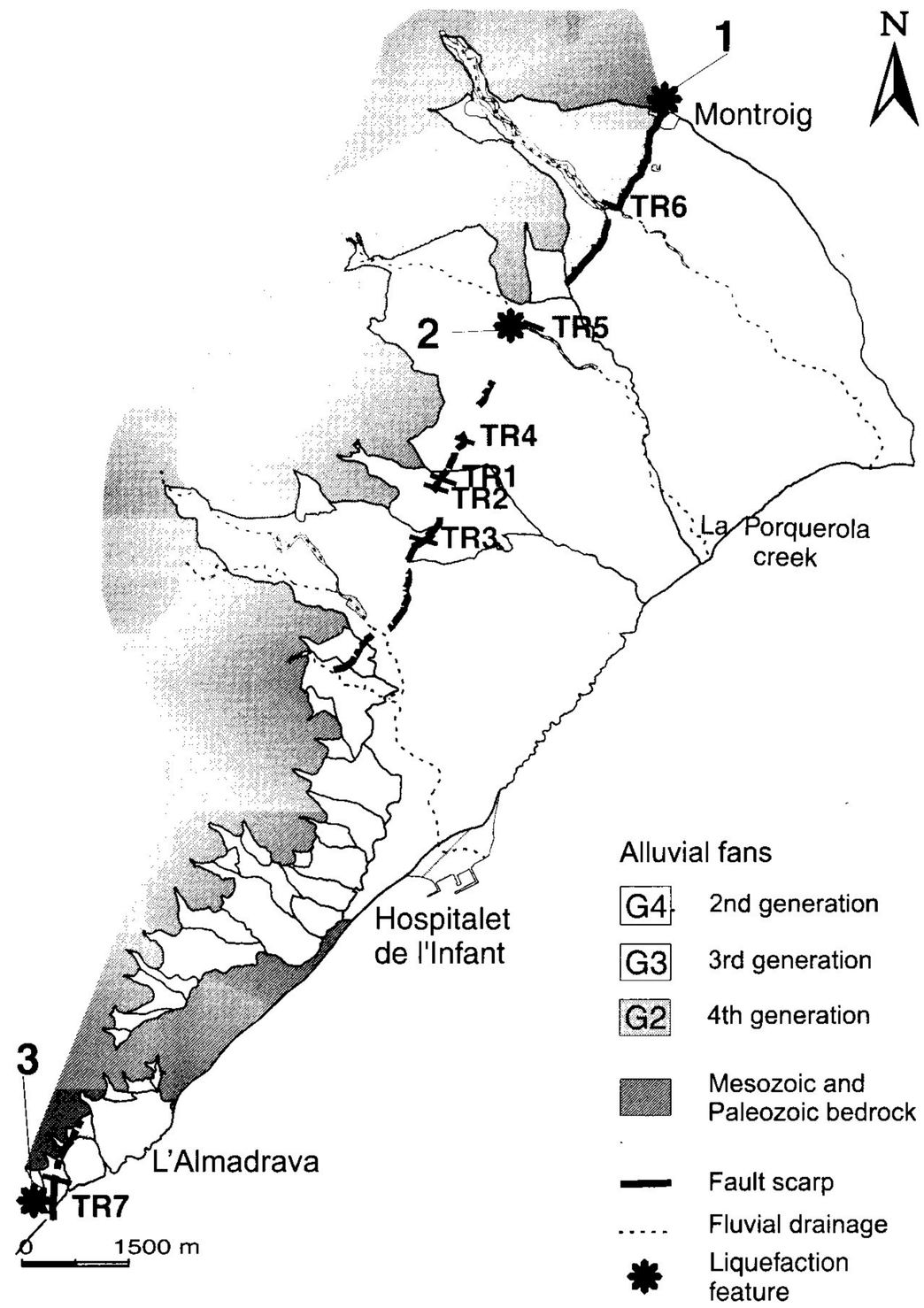

Fig. 3. Geomorphologic map of the studied area of the El Camp fault, south of Montroig. Simplified trace of the fault scarp cutting through three generations of alluvial fans are shown. Sites 1 to 3 where paleoseismic indicators are described in the text, Montroig, Porquerola and Almadrava sites, respectively.

Liquefaction features

The detailed mapping of the fault scarp in the field led to the detection of liquefaction features which were, in some cases, directly related to the fault. The most significant of these structures are close to the fault, but extensive liquefaction features were also found in Cap Roig (Fig. 1), several km southwest from the fault trace. A brief description of these structures is presented.

Porquerola site

The Porquerola creek (Fig. 3) is entrenched up to 10 m on a G3 alluvial fan (Fig. 4a). The top of the G3 layers, made up of high cemented conglomerates, corresponds to the 125000 yr old surface and is displaced by the fault. In the footwall of the fault, three sand dikes crop out at the creek wall cutting through a cemented conglomerate layer (layer 3) and are sealed by the gravel of layer 4 (Fig. 4a). The dikes, which dip approx. 60° (Fig. 4b-c), could have used preexisting joints corresponding to normal fractures caused by extension related to the fault activity. The fracture infilling is composed of matrix supported conglomerates (sandy matrix and very few pebbles) which were derived from the conglomerates that lie below the cemented conglomerates cut by the dike (Fig. 4b). The strike of the dikes is parallel to the general strike of the fault at this site (Fig. 4c, Porquerola plot). Given that the relationship between fracture infilling and its lower source is clearly exposed the dikes are interpreted as liquefaction features.

Almadrava site

At Almadrava, where the scarp enters the sea (Fig. 3), there are several liquefaction features located at less than 10 m from the fault. The most characteristic of these are on the fault scarp which, at this point, cuts through the G3 alluvial fans (Fig. 4d). The conglomerate layers are bent near the fault and several fractures parallel to the fault scarp were observed. Matrix supported conglomerates intrude upwards into the former conglomerate layer. The underlying layer is the source of the clastic dikes since the lithology is coincident. The dikes appear to be slightly more cemented than the source layer because of the water circulation or the difference in internal grain organization. Liquefaction is again the proposed explanation for these dikes. Moreover, some of the fractures slipped and acted as normal faults, creating metric fault scarps within the flexure. The sand dikes are parallel to the El Camp fault at this site (Fig. 4c-d, Almadrava plot) and also parallel to the open cracks measured in trench 7 situated several tens of meters to the north of this outcrop.

Cap Roig site

This site is located to the south of the El Camp fault, on the coast, north of the Ebro river delta (Fig. 2). It is the only site near the El Camp fault that contains extensive sediments suitable for liquefaction, i.e., non cemented fine sands near the topographic surface. Here these non cemented sands are inter-bedded with loose gravel made up of well classified rounded pebbles of fluvial origin (Ebro river). In some other outcrops along the terraces of the Ebro river, simple sand dikes intrude into the terrace gravel. At Cap Roig, a large number of sand dikes crop out on the Morro del Gos island (Fig 4e). This small island is composed of pre-Thyrrenian cross laminated sand-dunes deposited over the fluvial terrigenous and polygenic Ebro river deposits. Some of the fine sands and silts underlying the sand-dunes are clearly injected upwards (Fig. 4e) whether through joint planes trending NS and EW or through cross lamination planes. In addition to the sand dikes, several outcrops along the Morro del Gos beach and the railway reveal further liquefaction structures that can be classified as: 1) internal layer convolution including pillow structures, and 2) intrusion of sands into more cemented upper layers following fractures or lamination (Masana, 1996). Moreover, the outcrop shows a number of normal faults.

Montroig site

There is a vertical sand dike (Fig.3) which cuts through the cemented conglomerates belonging to the G2 alluvial fan generation in the footwall of the fault, only three meters away from the scarp-front. Several sub-vertical open cracks crop out next to it. The trend of the fracture that was used by the sand dike is parallel to the trends of the fault scarp and the open-cracks (Fig. 4c, Montroig plot). In this case, although the lower origin of the deposit which infills the dike was not identified, its strike and location with respect to the fault suggest a liquefaction origin as in the case of the aforementioned sites.

Liquefaction at the described sites can be directly related to the fault because the fractures involved are parallel to the fault and located close to it. The plots in fig.4 show this parallelism at each site. These fractures -some of them open cracks- could have played an important role in the location of the paths used by the liquefied material for transportation upwards

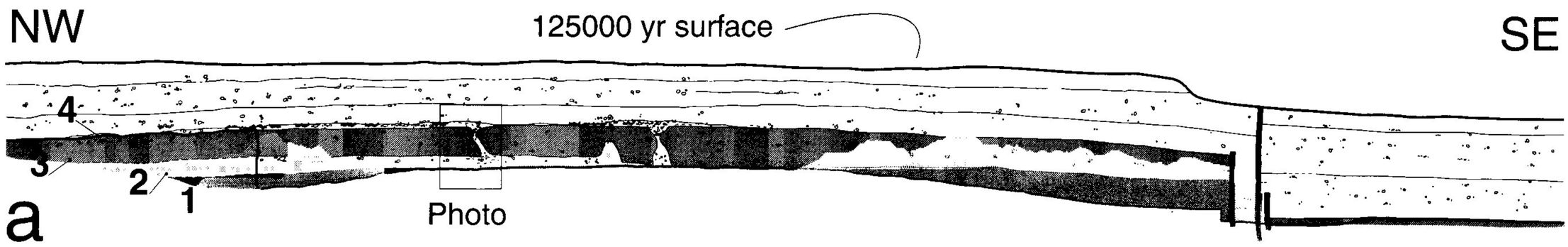

b

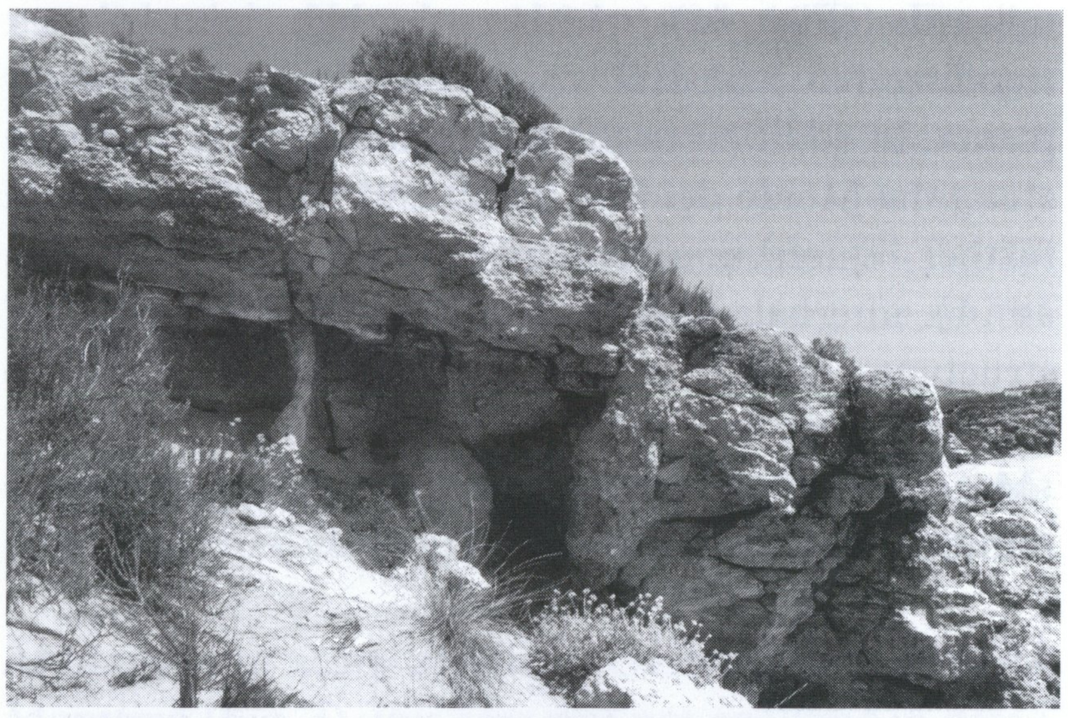

d

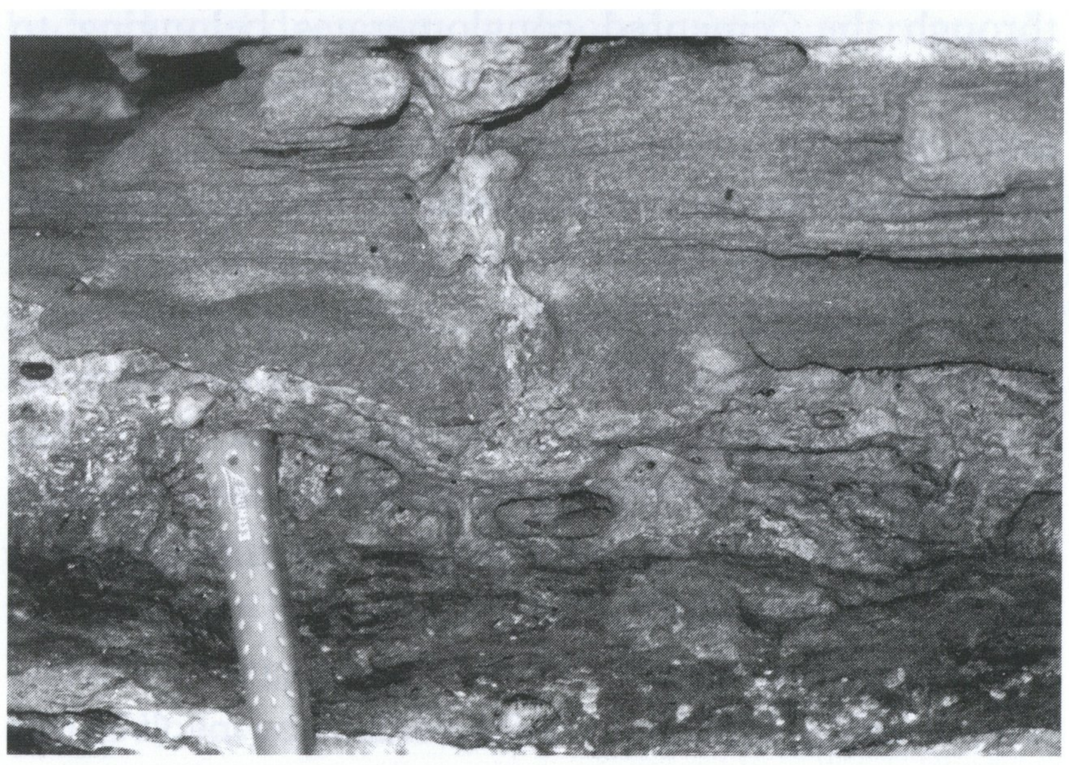

e

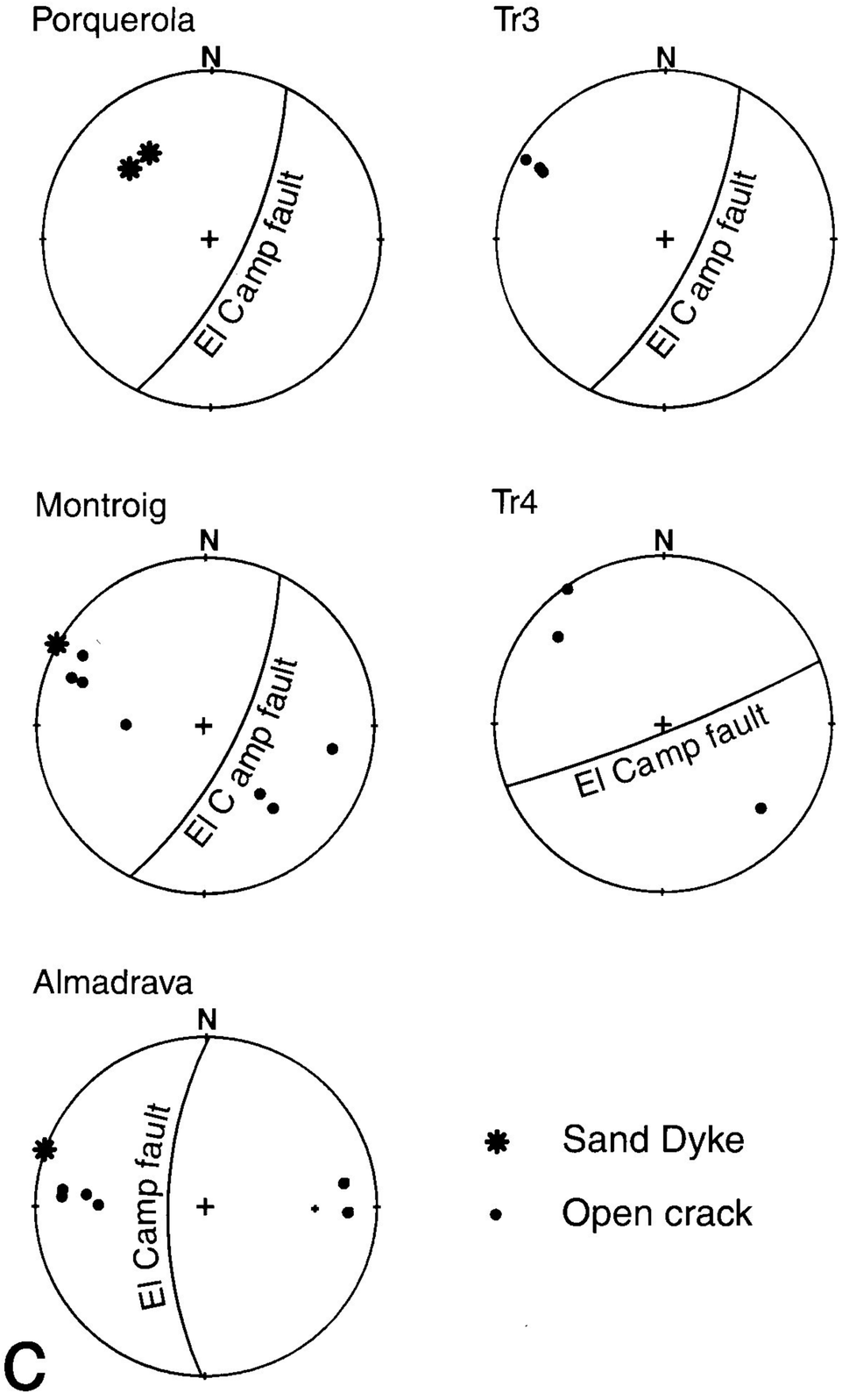

Fig. 4. Examples of the liquefaction features observed at different outcrops along the fault (located with stars in figure 3). a) Geologic profile of the Porquerola creek across the El Camp fault. See description in the text. b) Sand dike across a cemented conglomerate layer (layer 3). The infilling of the dike comes from the lower layer (layer 2) and is sealed by the upper gravel layer (layer 4). Situation in fig. 4a. c) Stereographic plots on the lower hemisphere of the El Camp fault at different sites and the liquefaction features observed together with the open crack data. d) Detail of the Almadrava outcrop with vertical clastic dikes crossing cemented conglomerates along the fault scarp. e) Sand dike of fluvial limes and sands injected into a sand dune deposit in the Cap Roig area (Morro del Gos island). Convolution is clear in the lower liquefied unit.

since the susceptibility to liquefaction of these sediments is low and the conglomerates covering them are strongly cemented. Given that this environment does not favor liquefaction features, the high pressure that is needed cannot be produced by the overlying layers as the outcrops are always located at less than 2 or 3 m below the fan surface. This suggests that seismic wave transmission could account for the pressure

required. Should this be the case, the shaking would have been significant as it reached Cap Roig, several kilometers west of the fault trace, with sufficient energy to produce pillow structures.

Trenching

Sites for trenching were initially selected where the fault scarp cut through the most recent alluvial sediments, i.e., through the G4 fans. Although the area has been modified by human activity, small parts of the scarp are still preserved. Trenches 1 and 2 were dug in the only preserved part of the scarp in the G4 fans, in a golf course. Trench 3 was dug in a slightly modified part of the scarp where the fault separates the G3 from the G4 alluvial fan sediments. Trench 4 was dug in a preserved area of a G3 alluvial fan cut by the fault scarp. Trenches 5 and 6 were not only dug for paleoseismological purposes but also to constrain the limits of the fault segments. This involved cleaning the banks of two creeks in order to see the upwards extent of the fault through the G3 unit. And finally, trench 7 already existed in the Almadrava area, at the southern edge of the scarp.

The boundaries of the different fans were determined in order to select the precise location of the trenches after a local geomorphologic analysis of the surroundings of the site. Furthermore, micro-topographic mapping and profiling were performed across the scarp, and mapping of the local geomorphologic units was carried out to select the areas with the best balance between erosion and deposition. Topographic profiling allowed us to quantify the vertical displacement of the deformed geomophologic surfaces.

The trenches were up to 40 m long and 5 m deep, and were mainly dug with a pneumatic drill as the alluvial fan conglomerates are usually cemented by calcrete soils. The trenches were analyzed in the standard way.

A number of dating methods were used for all the suitable samples in order to constrain the age of the events. Absolute dating was applied in samples of calcrete soils -U/Th (51 samples), Thermoluminiscence (35 samples)-, Charcoal, pollen and gasteropoda shells -Radiocarbon (8 samples). Pollen analysis was also performed in order to obtain chronological constraints and to correlate levels between the trenches (more than 60 analyzed samples). The results were carefully analyzed and many of them were rejected for a variety of reasons -contamination of the sample, sampling problems, incoherence with geologic constraints and between different dating methods-. Detailed discussion on the dating procedures can be found in Villamarín et al., (1999) and Santanach et al (2001).

Detailed description of each of the seven trenches is beyond the scope of this paper -see Masana et al. (2001, in press) and Santanach et al. (2001) for details on trenches. In this paper, we present the paleoseismic activity of the El Camp fault during the last 125000 yr BP., i.e. the seismic activity occurred after the deposition of the top layers of the G3 fan generation. The outcrops of trenches 5 and 6 (Masana et al. 2001, and Santanach et al. 2001) indicated that, from the Porquerola creek (trench 5) to the South, the El Camp fault ruptured the surface after 125000 yr BP, in contrast to the Rifà creek (trench 6) where the 125000 yr old surface was not ruptured by the fault. Thus a change in the fault behavior occurred between the Porquerola and Rifà creeks. Henceforth, we shall report only features observed to the south of the Porquerola creek, focussing our attention on the features which inform us about the seismic activity after 125000 yr BP. Only the southern walls of trench 1 and trench 4 are described since they show the necessary features for understanding the essential aspects of the paleoseismology south of the Porquerola creek.

Trench 1

This trench shows three fault zones cutting unit B, a highly cemented alluvial deposit (Fig. 5). The F1 and F2 faults consist of infilled open cracks (the real amount of opening is less than what can be measured in the log as the trench trend is not exactly perpendicular to the fault direction). In contrast to F1 and F3, F2 shows no evidence of vertical displacement. The overlying sediments (Unit C) are loose gravel of fluvial origin possibly transported by a small creek, which is located 10 m from the trench and incised in the footwall. Unit C seals the deformation created by F3 whereas unit D is deformed by F1. Unit E, which has a very local extension, is wedge shaped and composed of loose reddish fine-matrix gravel supporting some limestone cobbles. This unit, detected in the four walls of trenches 1 and 2, is not cut by F1, and is covered with the present soil (F).

Two deformation events were detected in this trench: 1) *event X*, which took place along F3 and F1 after the deposition of unit B and prior to unit C. Unit C buries the fault scarp at F3. 2) *event Z*, which occurred after the deposition of units C and D and prior to the formation of unit E. This unit developed at the expense of the re-uplifted fault scarp at F1 and was therefore, interpreted as a colluvial wedge. Based on the restoration of the deformation produced by these events a total vertical slip of 140 to 200 cm and 40-100 cm has been attributed to the events X and Z, respectively. See Masana et al. (2001) and Santanach et al. (2001) for further discussion.

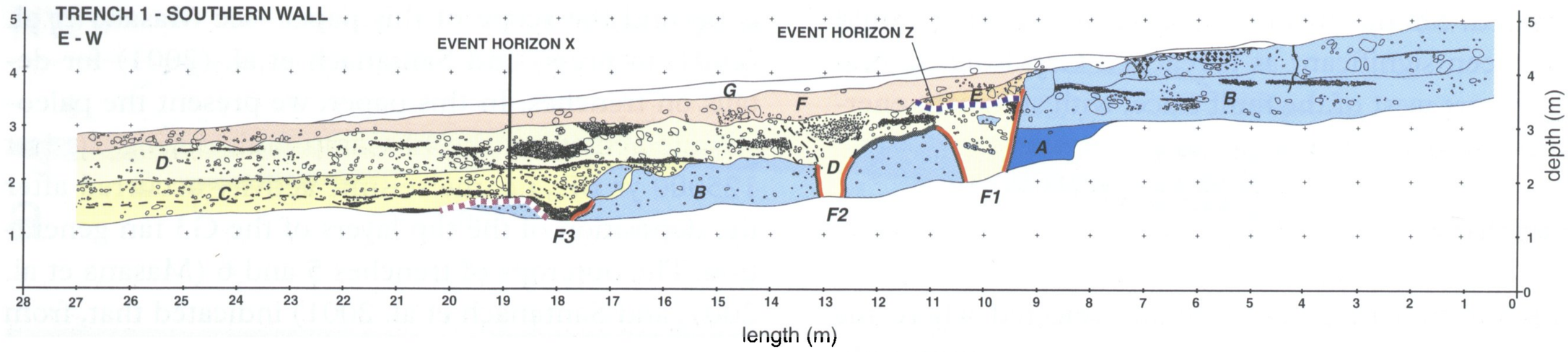

G Sand, anthropically deposited in relation to the golf course.

C Unconsolidated matrix-supported gravel. Clasts are carbonatic in composition, subrounded, moderately selected, and range from few millimeters to few decimeters in size. The matrix range from silty to sandy. The gravel show fluvial architecture.

F Silt and clay, dark brown in color, corresponding to the subcurrent soil. Scarce carbonatic, subrounded clasts ranging from few millimeters to few decimeters in size. $CaCO_3$ nodules.

B Strongly cemented and poorly selected matrix-supported conglomerates. Clasts are carbonatic, poorly classified, and range from few centimeters to few decimeters in size. The matrix range from silty to sandy and is yellowish in color. Decalcification processes occurred at the upper part of the unit. Extensive laminar caliche at top, and oolitic caliches inside the unit.

E Unconsolidated matrix-supported gravel. Clasts are carbonatic, subangular, and mainly centimeter-size, although some decimeter-size clasts are found close to the fault. Matrix range from clays to sands and is reddish brown in color. Presence of alive roots.

A Strongly cemented and poorly selected matrix-supported conglomerates. Clasts are carbonatic, poorly classified, and range from few centimeters to few decimeters in size. The matrix range from silty to sandy and is yellowish in color. Decalcification processes occurred at the upper part of the unit. Extensive laminar caliche at top, and oolitic caliches inside the unit.

D Unconsolidated matrix-supported gravel. Clasts predominate at the lower part of the unit, are carbonatic, subangular, and range from few millimeters to few decimeters in size. The matrix range from silty to sandy and is light brown in color.

Decalcified limestones

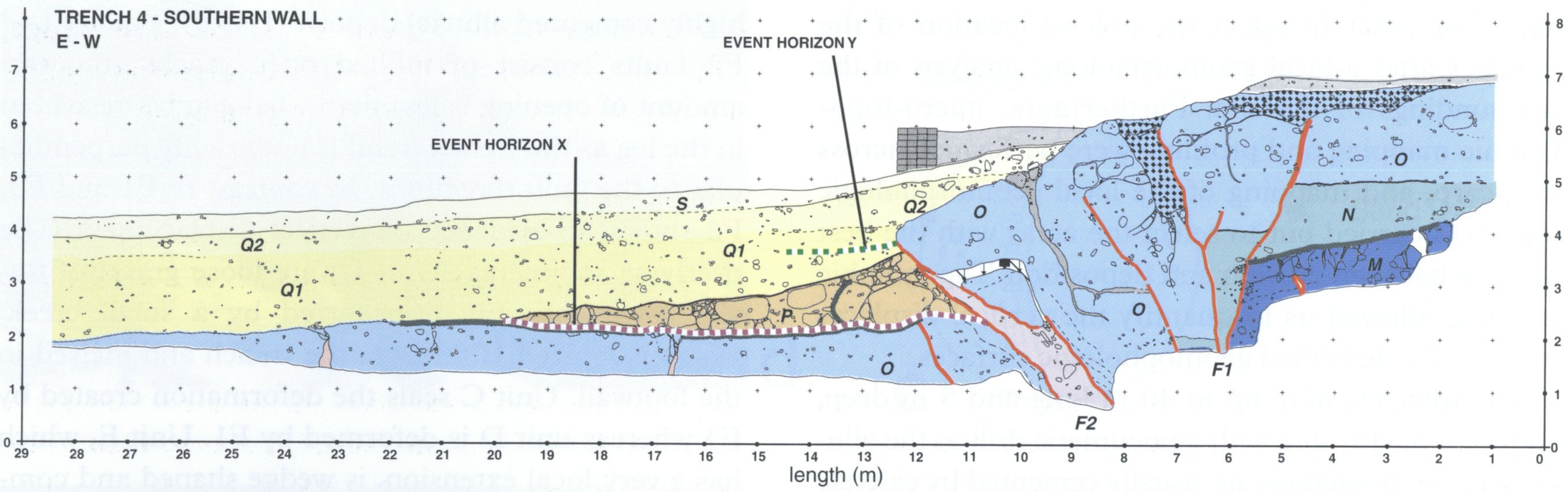

S Unconsolidated clays, dark brown in color, containing some clasts ranging from 2 to 10 cm in size. The upper part of the unit corresponds to the current soil.

O Strongly cemented, poorly selected, matrix-supported conglomerates. Clasts are carbonatic, subangular to subrounded, and range from few centimeters to few decimeters in size. Locally weathered at the top and along the joints. Laminar caliche at the top.

Q2 Unconsolidated, matrix-supported gravel. Clasts are very scarce. The matrix range from clays to silts.

N Unconsolidated, well selected silts and clays light brown -orange in color, including some decimeter-size, carbonatic clasts.

Q1 Slightly consolidated, matrix-supported gravel. Clasts are carbonatic, subangular, and moderately selected. The matrix range from clays to silts and is light brown in color.

M Highly cemented, matrix-supported conglomerates. Clasts are carbonatic, little selected, angular, and range from few centimeters to few decimeters in size. Matrix range from clay to silty and is pinky in color. Laminar caliche at the top. The north wall shows a clay-bed interlayered in the conglomerates. It is built up by light brown clays containing subangular clasts up to few centimeters in size.

P Moderately consolidated, heterometric, matrix-supported conglomerates. Clast are made of pieces of conglomerates showing facies corresponding to units O and M. Their size reaches up to 40 cm, and are strongly angular. The matrix range from clays to silts and is light brown in color.

Loose matrix-supported gravels with silty and sandy matrix.

Fig. 5. Logs of the southern walls of trenches 1 and 4.

https://doi.org/10.1017/S0016774600023854 Published online by Cambridge University Press

Dating of the calcrete soil on top of unit B in trenches 1 and 2 gives an age ranging between 80000 and 130000 yr BP. We interpret the top of unit B as corresponding to the top of the G3 fan generation which has been given an age of 125000 yr BP (Villamarín et al. 1999). The only dating method suitable for the fluvial deposits overlying unit B was pollen analysis. This does not result in an absolute age but allows us to correlate pollen contents and pollen associations of unit D with karstic infilling sediments in trench 2, containing charcoal dated with radiocarbon (31050+/-460 yr BP.). We suggest that a considerable amount of time elapsed since the occurrence of event X and the deposition of the dated material for the following reasons: 1) the correlated sample is in the upper part of unit D, and not at the bottom, 2) the thickness of unit C, between unit D and the top of the target horizon, and 3) the absence of the leached level which forms over calcrete horizons in association with their development. This indicates an erosion time between the formation of the calcrete and the deposition of unit C. Therefore, event X took place between 125000 yr and 31510 yr BP, but it is unlikely to have occurred close to the latter for the aforementioned reasons. Event Z took place after the deposition of unit D and a short time before the deposition of the colluvial wedge (Unit E). The lowest charcoal sample dated in unit E by Radiocarbon gives an age of 1102+/-93 yr AD. The age of event Z is constrained between 31510 yr BP and 1195 yr AD, but probably closer to the latter.

Trench 4

This trench shows a wide deformed area with two main faults (Fig.5). F1 dips towards the E while F2, the frontal fault, dips towards the W. According to the log of the northern wall of this trench (Masana et al., 2001, and Santanach et al. 2001) these two faults merge at depth. Next to F2 there are empty spaces and cracks that provide evidence of extension despite the fact that the fault has a reverse geometry. Both walls of the trench show a vertical offset of highly cemented alluvial conglomerates (Unit O) consistent with the fault scarp developed at surface. Adjacent to F2, in the hangingwall, there is a less cemented unit formed by large angular blocks of clast supported cemented conglomerate and a silty and sandy matrix, with a wedge shape (Unit P). This unit was interpreted as a colluvial wedge. Unit P is overlain by a series of loose and matrix supported gravel. (Units Q1, Q2 and S). The entire unit P and the lower part of unit Q1 are cut by F2.

A minimum of two deformation events were recognized in this trench. The older event triggered the formation of the colluvial wedge (Unit P) and thus took place immediately before it, and after the formation of the calcrete soil on the top of unit O. This is similar to event X in trenches 1 and 2. The younger event occurred during the deposition of unit Q1.

The top of unit O corresponds to the top of the G3 alluvial fan generation, which was given an age of 125000 yr BP (Masana et al., 2001 and Santanach et al., 2001). Thus the older event took place after this time. Although it was not possible to date the colluvial wedge with the result that the time constraints for this earthquake are imprecise, it is reasonable to correlate this event with event X of trenches 1 and 2. The younger event occurred during the deposition of unit Q1, which is largely pre-Holocene as this period of time is represented by unit S which contains Holocene pollen associations unlike Q2 and Q1. Therefore, the event represented by the rupture of the colluvial wedge and part of unit Q1 predates the Holocene and thus probably does not correlate with event Z in trenches 1 and 2, which was considered to have happened approx. 1195 yr AD. Hence, it was interpreted as an independent event: event Y.

The vertical offset created by event X can only be estimated by the thickness of the colluvial wedge, which is 140 cm and should be considered as a minimum. Event Y shows 40 cm of vertical offset.

Discussion

Evidence for the seismogenic behavior of the El Camp fault

Two kinds of evidence account for the seismogenic behavior of the El Camp fault: i) the described liquefaction features along the fault, and ii) the colluvial wedges observed in the trenches.

The wedge shaped units observed in the trenches present some particular characteristics which should be mentioned. These particularities are controlled by some specific environmental and geometrical conditions of the El Camp fault. This can be summarized as follows: 1) The highly cemented nature of the conglomerates, on top of which the 125000 yr old surface developed, prevents the fault scarp from rapid erosion given that the unit keeps its cohesion. 2) The high intensity of the $CaCO_3$ dissolution and the precipitation processes in the area result in the formation of large amounts of calcic soils and also karstification. Two consequences of these processes should be pointed out: the formation of red clayey layers where calcic carbonate has been leached from the surface to concentrate in lower root mats to form calcrete soils, and

the karstification processes of the cohesive conglomerates which also create red clays. 3) The E-dipping El Camp normal fault becomes vertical and even W-dipping when it reaches the surface. This implies local extension around the fault plane where it becomes vertical or W-dipping. Because of these characteristics two kinds of colluvial wedges are present (Fig. 6).

Type 1 colluvial wedge

Made up mainly of clast-supported conglomerates with small amounts of silty and sandy matrix and a large number of large angular blocks of highly cemented conglomerates. This is the case of the colluvial wedge observed in trench 4. This type of colluvial wedge develops in association with normal faults that show reverse fault geometry at surface. The local extension structures -open cracks and empty spaces- related to the reverse geometry of the fault at surface, together with pre-existing fractures in the uplifted wall of the fault due to earlier events provide the necessary instability for the scarp to collapse after the earthquake. As a result, a colluvial wedge deposit composed of large blocks of the former fault scarp cohesive conglomerates forms at the foot of the fault scarp. The angular shape of the blocks and the small amount of matrix suggest a rapid collapse of the coseismic newly formed scarp. Therefore, the age of the bottom of the colluvial wedge is practically the same age as the seismic event.

Type 2 colluvial wedge

This is composed of matrix supported gravel with a considerable amount of reddish silty and clayey matrix and a small number of pebbles and some cobbles with some evidence of dissolution processes on their surfaces. This is the case of the colluvial wedge developed after event Z in trench 1 (Fig.5). The wedge shape and its location next to the fault scarp of this deposit provide evidence of its origin related to the scarp formation. However, its composition does not correspond to the result of the fault scarp collapse since, in this case, the fault scarp is made up of cohesive conglomerates, and not of loose silts and clays, which is the composition of the matrix of the colluvial wedge. Only the small number of cobbles contained in the wedge can proceed directly from the 'in situ' scarp degradation. The red matrix was interpreted as being derived from the red karstic or pedogenic clays

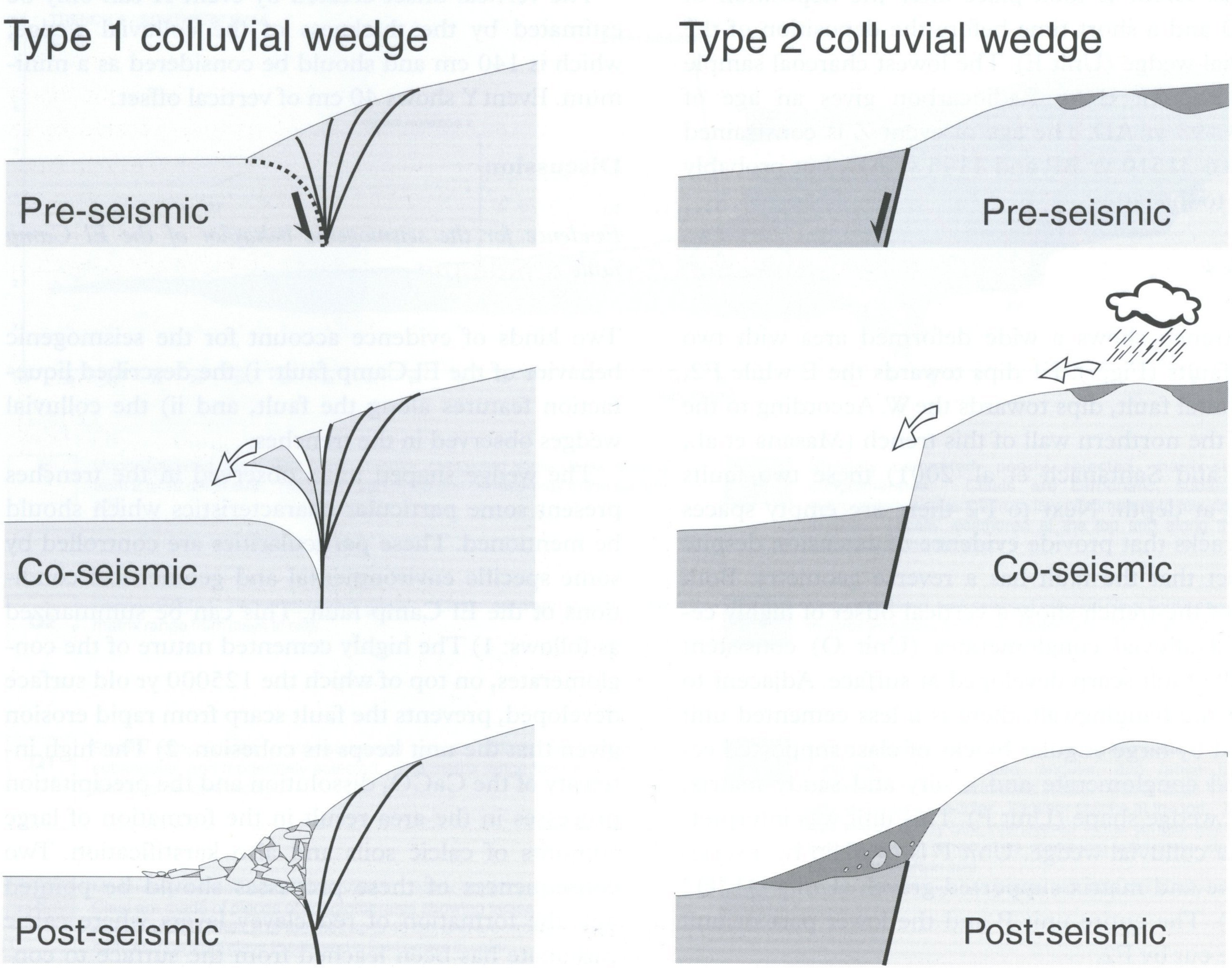

Fig. 6. Sketches showing the formation of the two kinds of colluvial wedges observed in the El Camp fault.

https://doi.org/10.1017/S0016774600023854 Published online by Cambridge University Press

formed from surface karstification or from the remains of the leached layer over the calcrete on top of the 125000 yr old surface. Water driven processes were responsible for the erosion, transport and deposition of these fine sediments in the small depocenter created by the seismic event at the foot of the fault scarp. This kind of colluvial wedge does not imply a sudden formation of the deposit after the earthquake. Therefore, the time between the earthquake and the bottom of the colluvial wedge may be longer than in type 1. Moreover, the type 2 colluvial wedge does not necessarily imply a seismogenic movement of the fault since the wedge can develop simultaneously with the slow growth of the scarp in a creeping fault. However, in the El Camp fault, the nature of type 1, suggesting a sudden formation of the colluvial wedge, together with the described liquefaction features related to the fault, provides evidence of the seismogenic behavior of the El Camp fault. Hence the type 2 colluvial wedge could also be related to seismically created scarps.

Paleoseismic results

The paleoseismic parameters of the El Camp fault are the following:

Seismogenic fault

Liquefaction features related to the fault and the nature of the colluvial wedges indicate that the El Camp fault is seismogenic.

Segmentation

The El Camp southern fault has two segments: to the north of the Porquerola creek, the fault ceased its activity between 300000 and 125000 yr, whereas to the south it continues to be active. The length of the southern segment is 14 km onshore and 10 km offshore, i.e., 24 km in total although it is not well constrained offshore.

Paleoearthquakes

Paleoseismic events were deduced from three kinds of evidence: colluvial wedges, broken colluvial wedges and buried scarps. Three events were described here in trenches 1 and 4 although there is evidence of some of them also in the remaining trenches (Fig. 7). Faulting prior to 125000 yr. BP was not considered in this discussion, since it was not possible to constrain the time bracket of its occurrence and its attribution to individual events of deformation.

The paleoearthequakes, which occurred after 125000 yr BP., are the following from young to old: Event Z) The evidence of this is a type 2 colluvial wedge (Fig.7). It created a 0.7 to 1 m high vertical displacement and took place in the interval between 30000 yr BP and 1195 yr AD, but with a high probability close to the latter as this is the age of the colluvial wedge base. Event Y) The evidence for this is a broken colluvial wedge. This created a 0.4 m high vertical displacement and postdates event X and predates the Holocene. Event X) The evidence for this is a colluvial wedge and a buried scarp. It created up to 1.4 m of vertical displacement in an individual event and up to 2 m in one or two different events, and occurred after 125000 yr and before 50000 yr. The vertical displacement observed in trench 1 for event X is

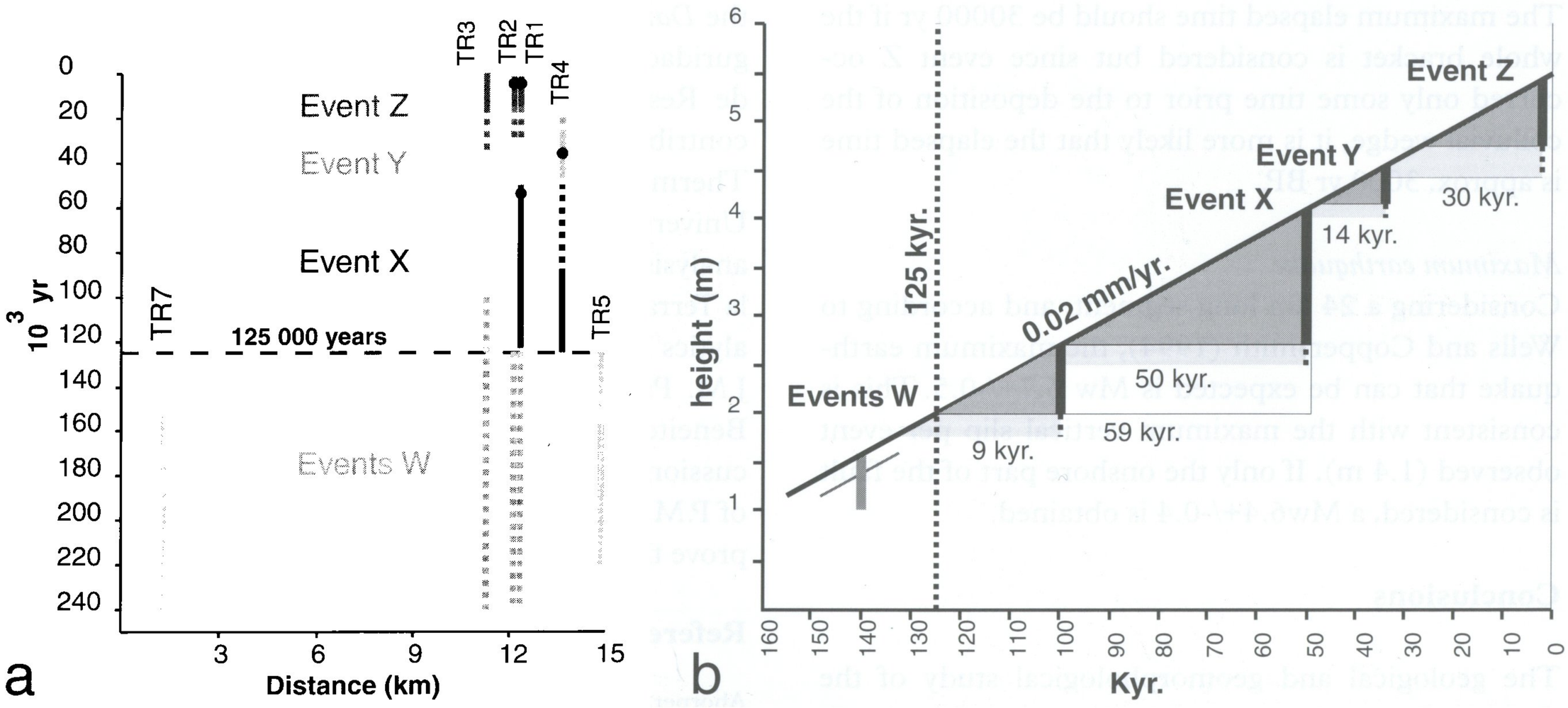

Fig. 7. a) Sketch of the events detected in the paleoseismological analysis and their age constraint. Events W are not described in the text as they were badly constrained in time. Black dot indicates the preferred time position for each event. b) Cumulative height versus time plot of the El Camp fault estimated from the paleoseismic results obtained. Estimated inter-seismic periods are also indicated.

twice the amount observed for event Z in this trench. This suggests two consecutive events after 125000 yr BP but prior to the deposition of unit C. This might imply a characteristic behavior of the fault. However, since in trench 4 the colluvial wedge, related to event X, is 1.40 cm thick, the two possible events would have a different slip.

Slip rate

The vertical slip rate of the fault was deduced from the vertical slip of the 125000 yr old surface. It was measured with microtopographic profiling across the scarp at different points. The vertical displacement of this surface is not regular. It ranges between 3.5 and 10.5 m, suggesting a slip rate between 0.02 and 0.08 mm/yr. In the trenches where the offset is high, there is evidence that the 125000 yr old calcrete developed over an older scarp. Because of this, 0.02 mm/yr, was considered to be a reasonable value for the slip-rate of the fault during the last 125000 yr.

Recurrence period

Evidence for three (four) events since 125 kyr has been obtained. If one or two different paleoearthquakes are considered for event X, the average inter-seismic period as shown in fig. 6 ranges between 34000 and 26000 yr. Considering that a vertical offset of 3.5 m in 125000 yr is reached by slips per event between 1 m and 0.7 m, the results obtained range between 25000 and 36000 yr. Hence the recurrence period is between these two values but, probably, based on the observation features, close to 30000 yr.

Elapsed time

The maximum elapsed time should be 30000 yr if the whole bracket is considered but since event Z occurred only some time prior to the deposition of the colluvial wedge, it is more likely that the elapsed time is approx. 3000 yr BP.

Maximum earthquake

Considering a 24 km long segment, and according to Wells and Coppersmith (1994), the maximum earthquake that can be expected is Mw 6.7+/-0.5. This is consistent with the maximum vertical slip per event observed (1.4 m). If only the onshore part of the fault is considered, a Mw6.4+/-0.4 is obtained.

Conclusions

The geological and geomorphological study of the Catalan Coastal Ranges allowed us to define the El Camp fault as an active seismogenic fault although it is a historically silent fault.

Two types of colluvial wedges were described along the cohesive El Camp fault scarp: type 1 corresponds to the collapse of the cohesive fault scarp when the normal fault has a reverse geometry at surface, and type 2 represents the erosion of red clays from carbonate leaching or karstification at the surface of the footwall. The seismogenic behavior of the El Camp fault is based on the existence of type 1 colluvial wedges and the liquefaction features related to the acceleration produced by the seismic activity.

The southern El Camp fault has two segments. The northern segment ceased its activity between 300000 yr BP and 125000 yr BP, whereas the southern segment has undergone three or maybe four large seismic events since 125000 yr BP. The southern segment has a slip rate of 0.02 mm/yr, an estimated recurrence period of 30000 yr, an elapsed time of 3000 yr and a maximum earthquake magnitude of Mw 6.7+/-0,5.

In general, it is possible, by means of geological analysis, to detect active faults, determine their seismogenic nature, and to characterize their seismic potential even where slip rates are low and no record of their seismicity exists in historical registers. The paleoseismological approach is a powerful and necessary tool for the accurate assessment of seismic hazard in regions with slow dipping active faults. This is the case in most parts of Western Europe, a highly populated and vulnerable region, where seismic hazard is underestimated given that it is calculated exclusively using the instrumental and historical catalogs.

Acknowledgments

This study was carried out under the framework of the *Datación* project co-funded by the Consejo de Seguridad Nuclear (CSN) and the Empresa Nacional de Residuos Radioactivos SA (ENRESA) with the contribution of Vandellós II Nuclear power plant. Thermoluminiscence dating was performed at the Universidad Autónoma de Madrid, U/Th and pollen analysis at the Institut Jaume Almera de Ciències de la Terra (CSIC), and Radiocarbon dating at Beta Analytics Inc. We thank Ramon Julià, Francesc Burjachs, J.M. Parés, Miguel Garcés, Tomás Calderón, Pedro Beneitez and Asunción Millán for their helpful discussions and contributions on dating. The comments of P.M. DeMartini and G.W. Michel helped us to improve the manuscript.

References

Ahorner, L., 1996. How reliable are speculations about large paleoearthquakes at the western border fault of the Roer Graben near Bree. Comptes Rendus des journées Luxemourgoises de géodynamique, 84: 39-55.

Anadón, P., Cabrera, L., Calvet, F. et al., 1983. El Terciario. *In*: I.G.M.E.(ed): Estudio geológico del Maestrazgo y de la mitad meridional de los Catalánides. 1-179.

Anadón, P., Colombo, F., Esteban, M. et al., 1979. Evolución tectonoestratigráfica de los Catalánides. Acta Geológica Hispànica, 14: 242-270.

Banda, E. and Correig, A.M. 1984., The Catalan earthquake of February 2, 1428. Engineering Geology, 20: 89-97.

Bartrina, M.T., Cabrera, L., Jurado, M.J., Guimerà, J., and Roca, E., 1992. Evolution of the central Catalan Margin in the Valencia trough (Western Mediterranean). Tectonophysics, 203: 219-247.

Camelbeeck, T. and Meghraoui, M., 1996. Large earthquake in Northern Europe more likely than once thought. Eos, 77 (42): 405-416.

Camelbeeck, T., Vanneste, K., Verbeeck, K. et al., 2001. Long-term seismic activity in the Lower Rhine Embayment. Cahiers du Centre Européen de Géodynamique et de Séismologie, 18, 35-38.

Fontboté, J.M., 1954. Las relaciones tectónicas de la depresión del Vallès-Pendès con la Cordillera Prelitoral y con la depresión del Ebro. Anonymous (ed): Tomo Homenaje al profesor E. Hernández Pacheco. Revista de la Sociedad Española de Historia Natural : 281-310.

Guimerà, J., 1984. Palaeogene evolution of deformation in the northeastern Iberian Pensinsula. Geological Magazine 121 (5): 413-420.

Julivert M, Fontboté JM, Ribeiro A, et al., 1972. Memoria explicativa del mapa tectónico de la Península Ibérica y Baleares. Madrid: I.G.M.E. 113 pp.

Maldonado, A., Alonso, B., Díaz, J.I. et al., 1986. Mapa geológico de la plataforma continental española y zonas adyacentes. Escala 1:200 000, Hoja nº 41-42 de Tortosa-Tarragona. Mem. expl. 78 p. Madrid. I.G.M.E.; 41-42.

Masana, E., 1994. El anàlisis de la red fluvial en el estudio de la neotectónica en las Cadenas Costeras Catalanas. *In*: Geomorfología en España Actas de la III Reunión de Geomorfología, Logroño. 1994; 29-41.

Masana, E., 1994. Neotectonic features in the Catalan Coastal Ranges, Northeastern Spain. Acta Geològica Hispànica. 29 (2-4): 107-121.

Masana, E., 1995. L'activitat neotectònica a les Cadenes Costaneres Catalanes. PhD thesis, University of Barcelona, 444 pp.

Masana, E., 1996. Evidence for past earthquakes in an area of low historical seismicity: the Catalan coastal ranges, NE Spain. Annali di Geofisica, XXXIX: 689-704.

Masana, E., Villamarín J.A. and Santanach, P., 2001. Paleoseismic results from multiple trenching analysis along a silent fault: The el Camp fault (Tarragona, northeastern Iberian Peninsula). Acta Geológica Hispànica, 36 (3-4): 329-354.

Nuñez, A., Colodrón, I., Ruiz, V., Cabañas, I. and Uralde, M.A., 1980. Mapa geologico de España, E. 1:50000 (Reus), Segunda serie, Mem. explic. Madrid, IGME, 33 p.

Sàbat, F., Roca, E., Muñoz, J.A. et al., 1997. Role of extension and compression in the evolution of the eastern margin of Iberia: the ESCI-Valencia Trough seismic profile. Revista de la Sociedad Geológica de España, 8 (1995) (4): 431-448.

Santanach, P., Masana, E. and Villamarín, J.A., 2001. Proyecto Datación, 160 pp. Consejo de Seguridad Nuclear, Madrid.

Villamarín, J.A., Masana, E., Calderón, T., Julià, R., and Santanach, P., 1999. Abanicos aluviales cuaternarios del Baix Camp (provincia de Tarragona): resultados de dataciones radiométricas. Geogaceta, 25: 211-214.

Wells, D.L. and Coppersmith, K.J., 1994. New empirical relationships among magnitude, rupture length, rupture width, rupture area, and surface displacement. Bull. Seism. Soc. Am., 84, 974-1002.